

# An Efficient Framework for Reliability Assessment of Power Networks Installing Renewable Generators and Subject to Parametric P-box Uncertainty

R. Rocchetta & E. Patelli

*Institute for Risk and Uncertainty, Liverpool University, United Kingdom*

**ABSTRACT:** In the last decades power grid is facing challenging problems due to the uncertain power output of renewable sources and environmental changes, which are drifting weather scenarios toward extremes. Problems of uncertainty are generally tackled by classical probabilistic approaches but in presence of imprecise data and scarce information they often require artificial assumptions hardly justifiable. Conversely, imprecise probabilistic frameworks have been recently developed to better deal with lack of data, epistemic uncertainty and contradictory sources of information, although are generally lacking in computational efficiency. This paper proposes an efficient reliability assessment framework that allows to study highly reliable power grid with distributed renewable sources which power outputs are modelled using parametric probability boxes. An adapted Importance Sampling algorithm is exploited to efficiently propagate the probability boxes and sample rare failure scenarios. The case study selected is a 6-nodes power network, modified to allocate renewable distributed generators. The approach is validated against Monte Carlo method. Furthermore, the efficient computational approach allows to conduce a sensitivity study over the imprecision sources, which would have been computationally intractable using brute force approaches. This allowed to identify which among the sources of imprecision affect the most the the failure probability estimate for the grid.

## 1 INTRODUCTION

Power grids are critical infrastructures designed with the primary goal of providing reliable electric power supply to the end-users and at the lower practicable cost. Traditionally, high capacity power generators were located far from the load points and are operated accordingly to a set of constraints, e.g. safety-related N-1 contingency constraint (Rocchetta, Li, & Zio 2015).

In the last decade the power grid original design has deeply changed. Nowadays it is common to see renewable and broadly distributed generators, which are generally located close to the electric power consumers. Those are often referred as Distributed Generators (DGs) and Renewable Energy Sources (RES). The DGs and RES are regarded as beneficial for the power grid because they can improve the grid voltage profile, mitigate power losses and cut green house gasses emissions. Nevertheless, an excessively high energy share from renewable sources can increase risks and drop power grid reliability. Those negative effects are mainly due to the uncertain power output of RES which depends on stochastic

weather conditions. Consequently the power demand variability increases and the available power capacity became less certain. This can lead to unexpected hazardous situations and drops in the overall power supply reliability, which in turn can increase the likelihood of large size and costly power outages.

Uncertainty can be generally classified in Aleatory and Epistemic uncertainty. The aleatory uncertainty refers to inherent randomness, stochastic behaviours and variability. It is considered not to be reducible even if further information is collected. On the other hand, epistemic uncertainty can be reduced and is used to explain lack of knowledge, imprecision and poor data quality. This classification of uncertainty sources is very convenient for the analysts, which can use it to quantify in which extent uncertainty is not reducible, due to aleatory uncertainty, and in which extent it might be reduced (i.e. epistemic uncertainty) if further data is collected.

Although classical uncertainty quantification frameworks are well-established and widely used, they might result in misleading conclusions if used when imprecision and severe uncertainty is affecting

the analysis (Beer, Ferson, & Kreinovich 2013). In fact, within an imprecise information scenario classical approaches may need strong initial assumptions (e.g. predefined probability distribution given just few samples) which are generally difficult to justify and can affect the goodness of the results. Imprecise probabilistic methods have been recently developed to rationally deal with imprecision and allows to perform the analysis with weaker assumptions and differentiating between epistemic and aleatory uncertainty.

Many works analysed the RES and DGs effect on power networks by mean of classical probabilistic approaches, e.g. Sansavini, Piccinelli, Golea, & Zio (2014), Rocchetta, Li, & Zio (2015), Mena, Hennebel, Li, Ruiz, & Zio (2014), Henneaux, Labeau, Maun, & Haarla (2016). These works applied probabilistic methods to characterize relevant sources of uncertainty and quantify their effects on the power grid costs, reliability and risks. Power grids are highly reliable systems and assess their failure probabilities can be time-consuming using classical methods (e.g. Monte Carlo simulations). The issue surely aggravates if imprecise probabilistic frameworks are employed, e.g. due to burdening computations (optimisations) to be performed in the probabilistic space on top of the probabilistic analysis.

In this paper, a model for reliability assessment of power grids allocating RES and DGs is presented and a criteria to define power network failure is introduced. The power output is modelled stochastically and some of the DGs (i.e. electric vehicles, storage systems) are assumed having an imprecisely known affects on the probabilistic model of the load demand (during charging times). Consequently, the parameters of the load probabilistic model are assumed as intervals and imprecise. An imprecise probabilistic framework is employed to perform uncertainty quantification and in order to reduce the computational costs an efficient algorithm is adapted from the one proposed by (Zhang 2012). The algorithm is used to speed-up the reliability bounds calculations and for the efficient propagation of parametric probability box. To conclude, a sensitivity analysis has been conducted over the sources of imprecision to identify the most relevant for the network reliability performance. Thanks to the developed framework, the sensitivity results are efficiently obtained and without the need of running a very high number of power flows.

In the paper, Section 2 proposes a concise review of uncertainty quantification approaches. The mathematical model used for power flow analysis, the probabilistic model and the framework for reliability assessment are presented in Section 3. A brief introduction on Importance Sampling method is also presented. Section 4 describes the proposed approach for

efficient reliability bounds estimation. The framework is tested on a power grid case study and results and discussion are summarized in Section 5. Section 6 concludes the paper.

## 2 UNCERTAINTY MODELLING BACKGROUND

When the analysis is affected by severe uncertainty or data is inconsistent or scarce, classical uncertainty quantification methods may require unwarranted assumptions to start the analysis, e.g. predefined probability distributions given small number of samples or subjectively assuming distribution families. Artificial model assumptions produce less robust solution or can even lead to misleading conclusions. To tackle this problem imprecise probabilistic frameworks and imprecise probabilistic theory have been developed to better deal with imprecision and lack of data using weaker or less assumption. Different methods and theories are discussed in literature (Beer, Ferson, & Kreinovich 2013) and some of the most intensively applied concepts are Evidence theory, interval probabilities, Possibility theory, level-two probabilistic approach, Fuzzy-based approaches and robust Bayesian approaches.

### 2.1 Probability Boxes

Probability boxes (P-boxes) are defined as a pair of CDFs bounding the probability between upper and lower bounds. P-boxes are popular mathematical tools often used to model quantities affected by both imprecision and aleatory uncertainty. Let first recall the definition of cumulative distribution functions (CDFs), which is a non decreasing mapping from  $\mathbb{R}$  to  $[0,1]$  such that for a probability measure  $P$  and for each  $p \in \mathbb{R}$ , the following  $F_P(p) = P((-\infty, p])$  holds. P-boxes is a pair of CDFs  $[\underline{F}, \overline{F}]$  such that  $\underline{F}$  stochastically dominates  $\overline{F}$  (Ferson, Kreinovich, Ginzburg, Myers, & Sentz 2002). It can be viewed as a continuous form of random sets as follows:

$$\{P \in \mathbb{P}_{\mathbb{R}} | \forall p \in \mathbb{R}, \underline{F}(p) = P((-\infty, p]) \leq \overline{F}(p)\} \quad (1)$$

where equation (1) define the credal set induced by the p-box  $[\underline{F}, \overline{F}]$ . For further theoretical details the reader is reminded to (Destercke, Dubois, & Chojnacki 2008)

P-boxes have been used in numerous applications to model variables affected by both Aleatory and Epistemic uncertainty, see for instance the works of (Feng, Patelli, Beer, & Coolen 2016). Distributional P-boxes and distribution-free P-boxes are two different types of P-boxes (Patelli, Alvarez, Broggi, & de Angelis 2014). For the first type, the underlying distribution family is well-known (e.g. Normal or Weibull) while its parameters are poorly known

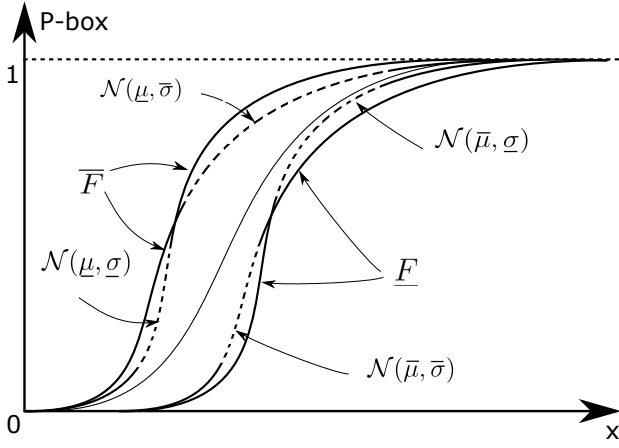


Figure 1: Example of distributional probability box. The family of the underlying distribution is normal and its standard deviation and mean are intervals  $[\underline{\sigma}, \bar{\sigma}]$  and  $[\underline{\mu}, \bar{\mu}]$ .

(i.e. just as confidence intervals). More generally, distribution-free P-boxes are defined only through bounds and the underlying probability distribution family is not known. In Figure 1 is depicted a distributional P-box, the probability distribution family is the normal distribution and its parameters  $\sigma$  and  $\mu$  are provided as intervals.

## 2.2 Uncertainty Propagation

Classical uncertainty propagation is commonly performed by means of Monte Carlo method or analogous techniques. First, input samples are randomly obtained by given probability distribution functions, e.g. by using the inverse CDF sampling method. Then, the samples are forwarded to the system solver which computes the output. Procedure is repeated and outputs probability distribution functions created. Uncertainty propagation for imprecise probabilistic frameworks (e.g. when P-boxes are used) can be done for instance by nested Monte Carlo method or by random sampling intervals directly from the P-box bounds (i.e. focal elements propagation). The focal elements propagation proceeds as follows. First, a so-called alpha-cut  $\alpha \sim U(0, 1)$  is sampled and intervals obtained as in equations (2)-(3).

$$\bar{F}_X(\alpha)^{-1} = \{x | \bar{F}_X(x) = \alpha\} \quad \forall \alpha \in [0, 1] \quad (2)$$

$$\underline{F}_X(\alpha)^{-1} = \{x | \underline{F}_X(x) = \alpha\} \quad \forall \alpha \in [0, 1] \quad (3)$$

Once intervals are sampled, the output bounds are obtained by solving minimization and maximisation problems (Patelli, Alvarez, Broggi, & de Angelis 2014) constrained by the sampled input intervals.

Generally speaking, the P-boxes uncertainty propagation procedure is time consuming and the output P-box tails might result poorly estimated due to lack of enough samples. This is a clear limitation in situations where the focus of the analysis is on the tails of

the output probability distribution, i.e. reliability estimation. This problem is going to be tackled in the rest of the paper.

## 3 POWER GRID MATHEMATICAL MODELLING

A power grid can be represented by a graph  $\mathcal{G}(\mathcal{N}, \mathcal{E})$ , let  $i$  denote nodes within the node set  $\mathcal{N}$  and be  $(i, j)$  the link between node  $i$  and  $j$  belonging to the line set  $\mathcal{E}$ . Let denote with  $N_l$  the number of loads, with  $N_g$  the number of generators in  $\mathcal{G}$ , with  $P_g$  the power injected by the generator  $g$ , with  $P_{i,j}$  the active power flowing in the line  $(i, j)$  and with  $\theta_{i,j}$  the voltage phase difference between nodes  $i$  and  $j$ .

In this work, a DC Optimal-Power-Flow (DC-OPF) is used as the solver for the power network economic dispatch problem. The economic dispatch problem is a cost minimization problem which primary goal is to determine the best power generators output which minimises the network cost. The optimisation problem is generally constrained by a set of physical (e.g. Ohm's law, power and current balances), operational (e.g. line thermal limit) and security-related constraints (e.g. N-1 contingency criteria). The DC power flow is regarded as a good approximation for power transmission system and it has been used also for distribution grid analysis (Mena, Hennebel, Li, Ruiz, & Zio 2014). Security constraints are neglected for simplicity. In this DC-OPF formulation, a load can be curtailed if needed. This has indeed very high cost for the grid and will occur only if the cost minimization problem can not be solved otherwise, e.g. if load demand exceeds the power capacity or to avoid line overloads.

The mathematical formulation is the following (Gan & Low 2014):

$$\min_{P_g, L_{cut}} f(P_g, L_{cut}) \quad (4)$$

where the cost function depends on the power generated and the load curtailed  $L_{cut}$ :

$$f(P_g, L_{cut}) = \sum_{g=1}^{N_g} C_g \cdot P_g + \sum_{i=1}^{N_l} C_{cut} \cdot L_{cut,i} \quad (5)$$

Subject to power generation constraints:

$$\underline{P}_g \leq P_g \leq \bar{P}_g \quad \forall g = 1, \dots, N_g \quad (6)$$

line flow constraints:

$$-\bar{P}_{i,j} \leq B_{i,j} \theta_{i,j} \leq \bar{P}_{i,j} \quad \forall (i, j) \in \mathcal{E} \quad (7)$$

and nodal active power balance constraints:

$$\sum_{g \in i} P_g + \sum_{j \neq i} B_{i,j} \theta_{i,j} + L_{cut,i} = L_i \quad \forall i \in \mathcal{N} \quad (8)$$

where  $C_g$  and  $C_{cut}$  are the cost per-unit of power for the generators and the load curtailed, respectively. The terms  $\underline{P}_g$  and  $\overline{P}_g$  are the minimum and maximum active power output of  $g$  and  $L_i$  is the aggregated load demanded at the node  $i$ .  $\overline{P}_{i,j}$  and  $B_{i,j}$  are the line  $(i, j)$  flow limit and susceptance, respectively. The voltage phase difference  $\theta_{i,j} = \theta_i - \theta_j$  is the difference between voltage phases at nodes  $i$  and  $j$ .

Renewable and other generators are considered as a set of possible technologies associated with the generator set. For instance:

$$P_g = \{P_{mg}, P_w, P_{pv}, P_{st}, P_{ev}\}$$

$$C_g = \{C_{mg}, C_w, C_{pv}, C_{st}, C_{ev}\}$$

where the subscripts refer to different generators technologies (g) such as main generators (mg), wind turbines (wt), photovoltaic panels (pv), storage systems (st) and electric vehicles (ev).

### 3.1 Classical Probabilistic Model: Weather and Components

A classical (precise) probabilistic model for DGs and RES technologies and for the weather conditions was presented in reference (Mena, Hennebel, Li, Ruiz, & Zio 2014) and reported here for completeness. The power injected into the grid by one wind turbine depends on the random wind speed and is determined as follows:

$$P_w(v) = \begin{cases} P_w^{ra} \frac{v - v_{ci}}{v_r - v_{ci}} & \text{if } v_{ci} \leq v < v_r \\ P_w^{ra} & \text{if } v_r \leq v < v_{co} \\ 0 & \text{otherwise} \end{cases} \quad (9)$$

where  $v_{ci}$  is the cut-in wind speed,  $v_r$  is the rated wind speed,  $v_{co}$  is the cut-out wind speed in [m/s] and  $P_w^{ra}$  is the rated power output for the turbine in per-unit of power. The wind speed  $v$  at time  $t$  is considered as a stochastic variable and it is assumed to follow a Rayleigh distributed as follows:

$$f_v(v) = \frac{v}{\sigma_v^2} e^{-\frac{v^2}{2\sigma_v^2}} \quad (10)$$

where fitting parameter  $\sigma_v$  can be estimated using historical data for the specific nodes or areas of the network.

The power of from a PV cell depends on the sun radiation  $s$  and on the PV cell parameters. The PV model is:

$$I = s \cdot (I_{sc} + k_i(T_c - 25)) \quad (11)$$

$$V = V_{oc} + k_v \cdot T_c \quad (12)$$

$$P_{pv}(s) = n_{cells} \cdot FF \cdot V \cdot I \quad (13)$$

where  $P_{pv}$  is the PV power output,  $n_{cells}$  is its number of cells,  $I_{sc}$  short circuit current,  $k_i$  current temperature coefficient,  $V_{oc}$  open circuit voltage,  $k_v$  voltage temperature coefficient. The expressions for the fill factor  $FF$  and the cell temperature  $T_c$  can be found in (Li & Zio 2012). The sun radiation  $s$  is assumed Beta distributed and its parameters  $a$  and  $b$  fitted on historical data and set equal to 0.26 and 0.73, respectively.

Storage systems and similarly electric vehicles can inject or withdraw electric power from the network nodes. Three EVs operating states have been considered, the vehicle to grid (V2G) the grid to vehicle (G2V) and the disconnected operative states. The discrete probability mass for EVs operative states  $f(t, op)$  is as follows:

$$f(t, op) = \begin{cases} p_{V2G}(t) & \text{if } op = V2G \\ p_{G2V}(t) & \text{if } op = G2V \\ p_{dcn}(t) & \text{if } op = \text{disconnected} \end{cases} \quad (14)$$

where  $p_{V2G}(t)$  is the V2G operative state probability at time  $t$ ,  $p_{G2V}(t)$  is the G2V operative state probability at time  $t$ ,  $p_{dcn}(t)$  is the probability of EV disconnected at time  $t$  and  $op$  is the EV operative state. The power injected or demanded by EVs ( $P_{ev}$ ) is equal to plus or minus the rated power  $P_{EV}^{rated}$  if the vehicle are in the discharging or charging states, respectively. If the random operative state result disconnected,  $P_{ev}$  is set to 0.

The state-of-charge ( $SOC_{st}$ ) for a package of storage devices is assumed uniformly distributed between 0 and the maximum capacity. The probability density function is as follows:

$$f_{st}(E_{st}) = \begin{cases} \frac{1}{E_S \cdot M_s} & \text{if } 0 \leq E_{st} \leq E_S \cdot M_s \\ 0 & \text{otherwise} \end{cases} \quad (15)$$

$$t_r = \frac{E_{st}}{P_{st}^{ra}} \quad (16)$$

$$P_{st}(t_r) = P_{st}^{ra} \quad (17)$$

where  $SOC_{st}$  is the storage state of charge,  $E_S$  is the specific energy of the active chemical,  $M_s$  is the total mass of the active chemical in the battery,  $P_{st}^{ra}$  is the rated power in [MW] and  $t_r$  is the discharging time interval considered to be 1 h.

In the work proposed by (Mena, Hennebel, Li, Ruiz, & Zio 2014), only discharge operative states

where considered, although is clear that storage charging can influence the load profile. In this work, this lack of information is shifted to the power demanded and the effects are incorporated into the probabilistic model of the loads.

### 3.2 Power Load Imprecise Probabilistic Model

The load demanded in each load bus can be regarded as an aggregation of random loads of lower magnitude. For instance, the load in a node  $i$  at a time  $t$  is the sum of residential and industrial loads, which in turn are the aggregation of smaller loads which also have some random behaviour. It is generally well-accepted hypothesis to consider aggregation of power loads normally distributed.

The imprecision surrounding the behaviour of power storages and electric vehicles is translated as uncertainty in the load demand profile. Thus, the loads for the nodes allocating ST devices are modelled as distributional P-boxes (because affected by both imprecision and aleatory uncertainty). The family of the distribution is assumed Normal and its parameters are known only as intervals. The P-box associated to the load demand at node  $i$  is defined as the following set of CDFs:

$$\{F_{L_i} \sim \mathcal{N}(\mu_i, \sigma_i), \underline{\mu}_i \leq \mu_i \leq \bar{\mu}_i, \underline{\sigma}_i \leq \sigma_i \leq \bar{\sigma}_i\}$$

Load demands in power grids are usually spatially and time correlated but for sake of simplicity, the correlation has been neglected in this analysis. Further model extensions will account for correlation between P-boxes using dedicated mathematical objects, e.g. copula structures.

### 3.3 Power Systems Reliability Index and Failure Criteria

In general terms, the probability of failures for a system can be defined as follows:

$$P_f = \int_{\Omega} f(\mathbf{x}) I(\mathbf{x}) d\mathbf{x} \quad (18)$$

where  $\Omega$  is the event space,  $f(\mathbf{x})$  is the joint probability distribution of the input  $\mathbf{x}$  and  $I(\mathbf{x})$  is the indicator function. The indicator function has value 1 for each  $\mathbf{x}$  leading to system failure and equal to 0 if not. In this work, the system fails if exceed predefined threshold level for the power network reliability index.

Generally speaking, many are the cases for which the integral in equation (18) has not closed from solution. An approximated solution can be obtained using Monte Carlo method:

$$\hat{P}_{f,MC} = \frac{\sum_{i=1}^{N_s} I(\mathbf{x}_i)}{N_s} \quad (19)$$

where  $N_s$  is the number of samples and  $\mathbf{x}_i$  is the  $i^{th}$  input sample vector. It is clear that the smaller the  $P_f$  the higher will be the  $N_s$  needed for its robust estimation. This is indeed a limitation of the Monte Carlo method, which clearly emerges when system to be evaluated is highly reliable or when the evaluation of the system status,  $I(\mathbf{x}_i)$ , is time-consuming (i.e. heavy computational model).

Importance sampling (IS) is a popular variance reduction technique used for efficiently estimate small failure probability. First, the importance distribution  $g(\mathbf{x})$  is selected and the equations (18)-(19) rewritten as follows:

$$P_f = \int_{\Omega} g(\mathbf{x}) \cdot \frac{f(\mathbf{x})}{g(\mathbf{x})} I(\mathbf{x}) d\mathbf{x} \quad (20)$$

$$\hat{P}_{f,IS} = \frac{\sum_{i=1}^{N_s} w(\mathbf{x}_i) I(\mathbf{x}_i)}{N_s} \quad (21)$$

where  $w(\mathbf{x}_i)$  are called importance weights computed as  $\frac{f(\mathbf{x}_i)}{g(\mathbf{x}_i)}$ . The importance distribution can be chosen arbitrarily and is generally selected in order to increase the frequency of samples which fall in the region of interest of the input space (i.e. the failure region). This allows estimating the failure probability as in equation (20) and reducing its variance. Select an appropriate  $g(\mathbf{x})$  is the critical step in the procedure. Practical recommendation is to select a  $g(\mathbf{x})$  easy to sample from and as close as possible to the original distribution  $f(\mathbf{x})$ . Different works discusses optimal selection for the importance distribution see for instance (Hu, Chen, Parks, & Yao 2016).

Many power grid reliability indices have been proposed, which are able to capture different features of the network. Indices such as Loss-of-Load-Probability (LOLP), System-Average-Interruption-Frequency-Index (SAIFI) and Energy-not-Supplied (ENS) are well-known and widely used. Here, ENS is adopted to quantify the amount of energy not provided to the customers over a fixes time window. It is computed as follows:

$$ENS = \sum_{t=1}^{T_h} \sum_{i \in \mathcal{N}} L_{cut,i,t} \cdot T_h \quad (22)$$

where  $T_h$  is the time window considered and  $L_{cut,i,t}$  is the load curtailed at each time  $t$  for each node  $i$  obtained as in equations (4)-(8).

In this work the indicator and failure region for the network is defined as:

$$I(\mathbf{x}) = \begin{cases} 1 & \text{if } ENS \geq ENS_{thr} \\ 0 & \text{otherwise} \end{cases} \quad (23)$$

where  $ENS_{thr}$  is the selected threshold level of energy not supplied, equal to a small percentage of the total load demanded by the network, i.e. 0.05 % of the total load  $\sum_{i \in \mathcal{N}} L_i$ . The network is considered in failure

if the energy not supplied exceed a predefined threshold level, that is  $ENS \geq ENS_{thr}$ . This is in line with a common practices in power grid reliability evaluations, sometime referred as the ‘one-day-in-ten-years’ criteria. This rule classifies power grids as reliable and unreliable when the average daily LOLP index is respectively lower or higher than 0.000274 (i.e. 1 day in 10 years).

#### 4 THE PROPOSED APPROACH

The method proposed for efficiently propagate parametric P-boxes is adapted from the algorithm introduced by Zhang (2012). The main difference is in the last step, where an optimisation strategy is employed. The optimisation is used to minimise and maximise the failure probabilities and avoid of over-conservatism problem of the original approach (Zhang 2012). The optimisation algorithm search among all the possible CDFs enclosed within the input p-box and select the one which minimises and maximises  $P_f$ .

The procedure is summarized as follows:

- **Step 1:** Using standard techniques, select the importance distribution  $g(\mathbf{x})$  for the power loads, set  $ENS_{thr}$  and the number of samples  $N_s$ ;
- **Step 2:** Sample  $N_s$  realizations from  $g(\mathbf{x})$  and the random variables for RESs and DGs  $\{s, v, op, E_{st}\}$ ;
- **Step 3:** For each sample  $\mathbf{x}_i$  solve DC-OPF, compute the  $ENS$  and obtain an indicator function  $I(\mathbf{x}_i)$ ;
- **Step 4:** Solve a minimization and maximisation problem constrained within the bounds of the vector of imprecise parameters  $\theta$ . The results are bounds on the failure probability as follows:

$$\underline{P}_f = \min_{\theta \leq \theta \leq \bar{\theta}} \left( \sum_{i=1}^{N_s} \frac{I(\mathbf{x}_i) f(\mathbf{x}_i, \theta)}{N_s g(\mathbf{x}_i)} \right)$$

$$\overline{P}_f = \max_{\theta \leq \theta \leq \bar{\theta}} \left( \sum_{i=1}^{N_s} \frac{I(\mathbf{x}_i) f(\mathbf{x}_i, \theta)}{N_s g(\mathbf{x}_i)} \right)$$

where  $f(\mathbf{x}_i, \theta)$  is the PDF value for the given  $\theta$  and  $\frac{I(\mathbf{x}_i)}{g(\mathbf{x}_i)}$  is retained from step 3.

The algorithm is efficient because the system solver has to run only  $N_s$  times for the IS method. Thus, the indicator function is retained and used within the minimization problem in Step 4 at very low computational cost. Conversely, the brute force

double loop Monte Carlo approach would need a considerably higher number of DC-OPF runs (i.e. the number of inner loop samples multiplied by the number of outer loop samples).

#### 5 CASE STUDY

The case study selected for the analysis is a 6-bus power network. The design data for the original system can be found in the MatPower (Zimmerman, Murillo-Sanchez, & Thomas 2011) study cases library under the name *case6ww*. Figure 2 displays the network topology, the nodes and load names and lines parameters such as maximum flows, resistances and reactances. DGs and RES generators have been allocated close to the load nodes and other modifications implemented as follows.

ST devices have been equally allocated in nodes 4-5-6 for a capacity equal to 7% of the node design load. One WT is allocated in node 4, EVs placed in nodes 5-6 and PVs cells in node 6. The maximum power output for the DGs is set equal to 70%, 3% and 2.7% of the original design load for WT, PV and EV respectively. The design load is incremented by a multiplying factor of 1.7 to counterbalance allocation of DGs. Due to DGs allocation, the mean of the load demanded in nodes 4-5-6 is imprecisely known. The load is assumed normally distributed and modelled as a distributional P-box, the parameter  $\mu$  is assumed to lay within the interval  $[0.95\mu, 1.05\mu]$  where  $\mu$  is the design load set to 119 MW (e.g. based on expert judgement). The standard deviation  $\sigma$  assumed equal to 11.9 MW (e.g. estimated from historical data).

##### 5.1 Result and Discussion

First, a comparison study between Monte Carlo method and Importance Sampling method is carried out to test the goodness of the second approach. The epistemic uncertainty on the load  $\mu$  is neglected by fixing its value to 119 MW for each node (i.e. design

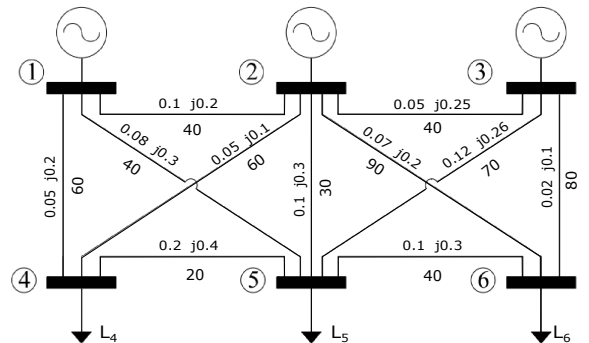


Figure 2: The 6-bus power grid topology. On top of each line are displayed resistance and reactants and on the bottom, the maximum allowed flow in per unit.

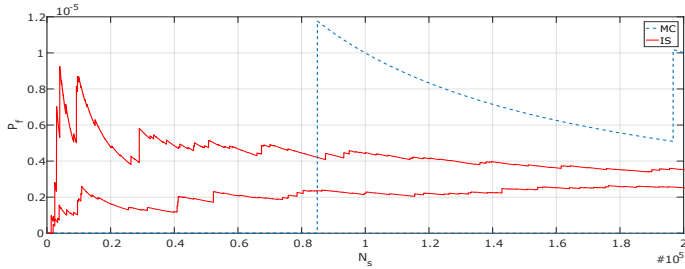


Figure 3: Comparison between two independent runs for Importance sampling (red solid line) and MC (blue dashed lines) methods. The plot shows convergence plot for the expected probability of failure  $P_f$  against the number of samples  $N_s$ .

load increased of factor 1.7). The importance distribution  $g(\mathbf{x})$  is selected by increasing the standard deviation of the loads from 11.9 to 13.1 MW which allows sampling more scenarios with high load.

Figure 3 shows the convergence curves for  $\hat{P}_f$  using two independent Monte Carlo and Importance Sampling runs for different numbers of samples. It can be observed that MC (blue dashed lines) is not efficient in sampling failure scenarios, which affect the goodness of the  $P_f$  estimator. The  $\hat{P}_f$  values obtained by MC method are 0 and  $10^{-5}$  for the first and second run, respectively. On the other hand, the IS method (red solid lines) allows improving the estimation of  $P_f$  reducing its variance. The resulting  $\hat{P}_f$  is about  $0.25 \cdot 10^{-5}$  and  $0.35 \cdot 10^{-5}$  for first and second run, respectively. The overall computational time for MC or IS is about 28.8 minutes on a machine installing an Intel Core 2.00 GHz processor and 8.00 Gb RAM.

After the verification of the IS approach, it has been applied also accounting imprecision to the load mean value at each node. At each load node, the interval  $[0.95\mu, 1.05\mu]$  is considered, where  $\mu$  is the design mean load. The IS algorithm is applied and failure probability bounds are  $\bar{P}_f = 1.296 \cdot 10^{-4}$  and  $\underline{P}_f = 3.6 \cdot 10^{-8}$  (the first row of Table 1). It must be observed that the overall computational time for the reliability bound analysis is the sum of the time need to perform the IS algorithm plus the time needed to solve the optimisation problem. The time needed to perform optimisation is fairly low because the DC-OPF is not called within the optimisation procedure. For instance, using a genetic algorithm optimizer  $10^5$  IS samples and 10 generation the overall time for minimization and maximisation is about 72 seconds on the cited machine.

The obtained  $P_f$  bounds are compared to brute force double loop MC solution. The epistemic variables are sampled in the outer loop (i.e. the load  $\mu$ ) while a classical MC is nested to the previous (i.e. inner loop). The samples obtained in the outer loop were just 10 due to time constraints, and the bounds computation took about 4.5 hours on the standard machine. The very rough estimations for the bounds are

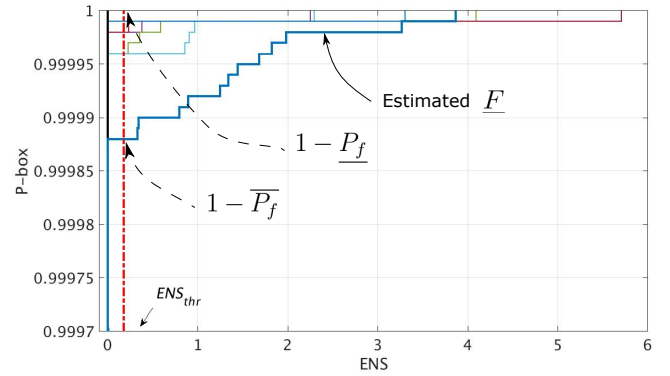


Figure 4: The result of double loop MC approach, the P-box of the ENS. The figure is zoomed on the right tails to improve visual outputs. The  $ENS_{thr}$  is displayed with dashed red line and the reliability bounds estimators computed as displayed.

Table 1: The result of sensitivity analysis obtained reducing the imprecision associated with the mean value of the load demand one-at-a-time.

	$\underline{P}_f \cdot 10^{-8}$			$\bar{P}_f \cdot 10^{-4}$		
Imprecision	$L_4$	$L_5$	$L_6$	$L_4$	$L_5$	$L_6$
$[0.95\mu, 1.05\mu]$	3.6	3.6	3.6	1.296	1.296	1.296
$[0.96\mu, 1.04\mu]$	9.6	3.6	3.7	0.675	1.299	1.292
$[0.97\mu, 1.03\mu]$	24.4	3.6	3.7	0.340	1.304	1.287
$[0.98\mu, 1.02\mu]$	60.3	3.6	3.8	0.165	1.309	1.282
$[0.99\mu, 1.01\mu]$	143.3	3.6	3.8	0.077	1.315	1.276
$[\mu, \mu]$	328.6	3.6	3.8	0.035	1.321	1.271

$\bar{P}_f = 1.2 \cdot 10^{-4}$  and  $\underline{P}_f = 0$ , similarly to the IS results. The ENS P-box has been plotted in Figure 4 and zoomed on the tail for better graphical resolution. It can be noticed that tails are coarsely estimated due to the low number of samples and the high system reliability.

### 5.1.1 Sensitivity Analysis

The figure 5 depicts sensitivities of  $\bar{P}_f$  (top plot) and  $\underline{P}_f$  (bottom plot) due to progressive reduction in the mean load imprecision. The sensitivity has been performed by shrinking the bounds on the loads  $\mu$  one-at-a-time. The reliability bounds changes due to reduction in the imprecision on  $L_4, L_5$  and  $L_6$  is displayed in Table 1. It can be observed that  $\bar{P}_f$  reduces (top plot) and  $\underline{P}_f$  increases (bottom plot) when  $L_4$  progressively became more precise (red dashed line). On the other hand, the considered level of imprecision on the mean value of  $L_5$  and  $L_6$  affects slightly the reliability bounds results.

It is clear that  $L_4$  reduces the most the reliability bounds if compared to  $L_5$  and  $L_6$ . In fact, if the interval (i.e. imprecision) associated to  $\mu_4$  shrinks from the wider  $[0.95\mu_4, 1.05\mu_4]$  to a crisp value  $[\mu_4, \mu_4]$ , then the estimated  $\underline{P}_f$  goes from about  $3.5 \cdot 10^{-9}$  to about  $4.5 \cdot 10^{-7}$  and  $\bar{P}_f$  from about  $3 \cdot 10^{-5}$  to  $3 \cdot 10^{-7}$  (see Table 1). This is the most relevant sources of imprecision and better specify its probabilistic model would provide the higher benefit (i.e. system reliability performance more precise). This high sensitivity to  $L_4$

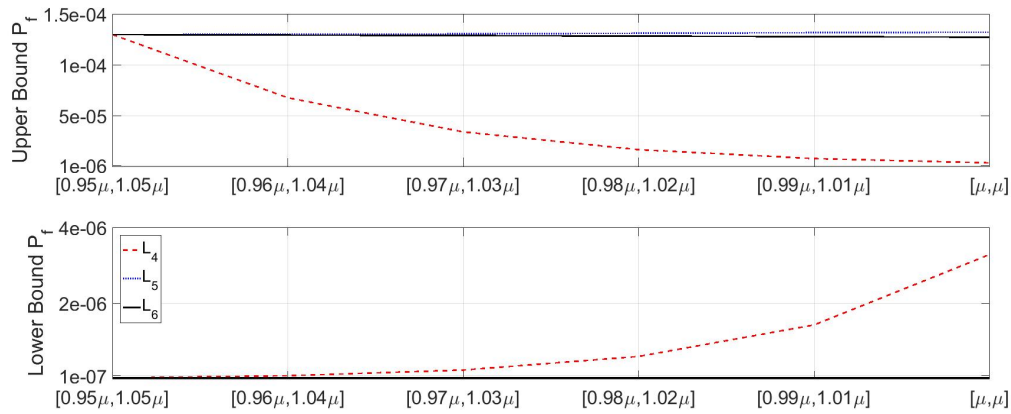


Figure 5: Sensitivity on the network upper failure probability bound (top figure) and the lower bound (bottom figure) due to the shrinking of imprecision interval on the mean load 4, load 5 and load 6 taken one-at-a-time.

is probably due to the maximum allowed to flows of links connected to node 4. In fact, the lines (1, 4), (2, 4) and (4, 5) have maximum capacity of 60, 60 and just 20 MW of power, respectively. In particular, line (4, 5) acts as bottleneck for the network, which has to curtail part of  $L_4$  load in order to satisfy operational constraints on  $\bar{P}_{i,j}$ , see constraints in equations 7. Conversely, reducing the imprecision on the mean loads at nodes 5 (red dotted line) and 6 (black solid line) does not significantly alter the epistemic uncertainty (i.e. interval) of the failure probability. In Table 1 are summarised the results of the sensitivity analysis.

## 6 CONCLUSIONS

A framework for efficient reliability assessment of power grids subjects to parametric P-box uncertainty is presented. The framework has been used to assess the energy not supplied by a DGs network and to assess the imprecision on its probability of failure. The adopted computational strategy makes use of an importance sampling algorithm embedded within an imprecise probabilistic framework for advanced uncertainty quantification. This allows to speed up the computations and to propagate distributional P-boxes by retailing DC-OPF simulations. This makes the framework fast and flexible enough to perform sensitivity analysis on the system failure probability. Sensitivity analysis allowed to point out the most relevant sources of imprecision with a relatively low computational demand.

## ACKNOWLEDGEMENT

This research project has been conducted within institute for Risk and Uncertainty at Liverpool University and sponsored by EPSRC and ESRC.

## REFERENCES

Beer, M., S. Ferson, & V. Kreinovich (2013). Imprecise probabilities in engineering analyses. *Mechanical Systems and Signal Processing* 37(1-2), 4–29.

Destercke, S., D. Dubois, & E. Chojnacki (2008). Unifying practical uncertainty representations i: Generalized p-boxes. *International Journal of Approximate Reasoning* 49(3), 649 – 663.

Feng, G., E. Patelli, M. Beer, & F. P. Coolen (2016). Imprecise system reliability and component importance based on survival signature. *Reliability Engineering & System Safety* 150, 116 – 125.

Ferson, S., V. Kreinovich, L. Ginzburg, D. S. Myers, & K. Sentz (2002). *Constructing probability boxes and Dempster-Shafer structures*, Volume 835. Sandia National Laboratories.

Gan, L. & S. H. Low (2014, Nov). Optimal power flow in direct current networks. *IEEE Transactions on Power Systems* 29(6), 2892–2904.

Henneaux, P., P. E. Labeau, J. C. Maun, & L. Haarla (2016, May). A two-level probabilistic risk assessment of cascading outages. *IEEE Transactions on Power Systems* 31(3), 2393–2403.

Hu, X., X. Chen, G. T. Parks, & W. Yao (2016). Review of improved monte carlo methods in uncertainty-based design optimization for aerospace vehicles. *Progress in Aerospace Sciences* 86, 20 – 27.

Li, Y. & E. Zio (2012). Uncertainty analysis of the adequacy assessment model of a distributed generation system. *Renewable Energy* 41, 235 – 244.

Mena, R., M. Hennebel, Y.-F. Li, C. Ruiz, & E. Zio (2014). A risk-based simulation and multi-objective optimization framework for the integration of distributed renewable generation and storage. *Renewable and Sustainable Energy Reviews* 37, 778 – 793.

Patelli, E., D. A. Alvarez, M. Broggi, & M. de Angelis (2014). An integrated and efficient numerical framework for uncertainty quantification: application to the nasa langley multidisciplinary uncertainty quantification challenge. *16th AIAA Non-Deterministic Approaches Conference*, 2014–1501.

Rocchetta, R., Y. Li, & E. Zio (2015). Risk assessment and risk-cost optimization of distributed power generation systems considering extreme weather conditions. *Reliability Engineering & System Safety* 136(0), 47 – 61.

Sansavini, G., R. Piccinelli, L. Golea, & E. Zio (2014). A stochastic framework for uncertainty analysis in electric power transmission systems with wind generation. *Renewable Energy* 64, 71 – 81.

Zhang, H. (2012). Interval importance sampling method for finite element-based structural reliability assessment under parameter uncertainties. *Structural Safety* 38, 1 – 10.

Zimmerman, R. D., C. E. Murillo-Sanchez, & R. J. Thomas (2011, Feb). Matpower: Steady-state operations, planning, and analysis tools for power systems research and education. *IEEE Transactions on Power Systems* 26(1), 12–19.